Integrated Genomic Profiling of Chronic Lymphocytic Leukemia Identifies Subtypes of Deletion 13q14

Peter Ouillette,[1] Harry Erba,[1] Lisa Kujawski,[1] Mark Kaminski,[1] Kerby Shedden,[2] and Sami N. Malek[1]

[1]Department of Internal Medicine, Division of Hematology and Oncology and [2]Department of Statistics, University of Michigan, Ann Arbor, Michigan

Abstract

Chronic lymphocytic leukemia (CLL) is a biologically heterogeneous illness with a variable clinical course. Loss of chromosomal material on chromosome 13 at cytoband 13q14 is the most frequent genetic abnormality in CLL, but the molecular aberrations underlying del13q14 in CLL remain incompletely characterized. We analyzed 171 CLL cases for loss of heterozygosity and subchromosomal copy loss on chromosome 13 in DNA from fluorescence-activated cell sorting–sorted CD19$^+$ cells and paired buccal cells using the Affymetrix *Xba*I 50k SNP array platform. The resulting high-resolution genomic maps, together with array-based measurements of expression levels of RNA in CLL cases with and without del13q14 and quantitative PCR–based expression analysis of selected genes, support the following conclusions: (*a*) del13q14 is heterogeneous and composed of multiple subtypes, with deletion of *Rb* or the *miR15a/miR16* loci serving as anatomic landmarks, respectively; (*b*) del13q14 type Ia deletions are relatively uniform in length and extend from breakpoints close to the *miR15a/miR16* cluster to a newly identified telomeric breakpoint cluster at the ~50.2 to 50.5 Mb physical position; (*c*) LATS2 RNA levels are ~2.6-fold to 2.8-fold lower in cases with del13q14 type I that do not delete *Rb*, as opposed to del13q14 type II or all other CLL cases; (*d*) PHLPP RNA is absent in ~50% of CLL cases with del13q14; and (*e*) ~15% of CLL cases display marked reductions in *miR15a/miR16* expression that are often but not invariably associated with bi-allelic *miR15a/miR16* loss. These data should aid future investigations into biological differences imparted on CLL by different del13q14 subtypes. [Cancer Res 2008;68(4):1012–21]

Introduction

Chronic lymphocytic leukemia (CLL) is the most common form of adult leukemia in the Western world and is characterized by a highly variable clinical course (1). Genetic subtypes of CLL that display different biological and clinical properties have been identified (2–5).

Fluorescence *in situ* hybridization (FISH) has identified various chromosomal changes, including del13q14, in ~80% of patients with CLL, and the presence of specific chromosomal abnormalities has proved to be a prognostic indicator for disease progression and survival (6).

Loss of chromosomal material, including the genomic marker D13S319 on chromosome 13 (known as the deletion 13q14), occurs in ~50% of all CLL cases and multiple other cancers (7, 8). Efforts by multiple groups have identified candidate genes within an ~1 Mb stretch on chromosome 13 that have each been implicated in CLL del13q14 biology; nonetheless, mutations in these genes have not been identified and questions remain as to the validity of reducing the biology of del13q14 to a minimal deleted region or a single-gene mutation/expression event (8–19). Analysis of del13q14 is further complicated by an evolving understanding of resident gene structure and the discovery of complex noncoding RNAs (20).

Given the absence of mutations in genes within del13q14, haploinsufficiency has been proposed as a mechanism of action (21). However, independent experimental verification for such a mechanism has not yet been reported.

More recently, discovery of the deletion or reduced expression of two microRNAs *miR15a* and *miR16* as part of del13q14 has been suggested as a unifying principle underlying del13q14 pathogenesis (22). Searches for miR15a/miR16 targets have identified Bcl-2 mRNA, and data have been presented in heterologous cell lines that suggest Bcl-2 mRNA regulation by these miRs (23).

Nonetheless, the general favorable outlook for patients with del13q14 remains difficult to reconcile with the postulated consequences of *miR*-locus deregulation/deletion, as patients with CLL and high Bcl-2 levels tend to have more aggressive disease (24).

Given the frequent occurrence of del13q14 in multiple cancers and given some of the abovementioned uncertainties surrounding its biology, we decided to analyze this lesion using high-resolution genomic mapping efforts.

Herein, we report the results of a large CLL profiling study with focused analysis of deletion 13q14 using 50k Affymetrix SNP microarrays (25) resulting in the identification of subtypes of del13q14 based on anatomic and functional criteria. Furthermore, we report that ~15% of CLL cases display marked reductions in *miR15a/miR16* expression that are often but not invariably associated with bi-allelic *miR15a/miR16* loss (26).

SNP array data were integrated with expression data and led to the discovery of differential expression of *LATS2* in del13q14 subtypes. Finally, expression of *PHLPP* was lower and often undetectable in del13q14 CLL cases as opposed to other FISH-based genomic CLL subgroups (27).

Materials and Methods

Patients

Between January 2005 and July 2007, 179 CLL patients evaluated at the University of Michigan Comprehensive Cancer Center were enrolled onto this study. Eligibility criteria required a diagnosis of CLL based on the

Note: Supplementary data for this article are available at Cancer Research Online (http://cancerres.aacrjournals.org/).

Requests for reprints: Sami N. Malek, Department of Internal Medicine, Division of Hematology and Oncology, University of Michigan, 1500 E. Medical Center Drive, Ann Arbor, MI 48109-0936. Phone: 734-763-2194; Fax: 734-647-9654; E-mail: smalek@med.umich.edu.

doi:10.1158/0008-5472.CAN-07-3105

National Cancer Institute Working Group Guidelines (28). We validated that the diagnostic criteria were met for all subjects through review of both laboratory (complete blood count with differential) and pathology (flow cytometry, bone marrow biopsy/aspirate, lymph node biopsy) reports dated at the time of diagnosis. Eligible patients needed to have an absolute lymphocytosis (>5,000 mature lymphocytes/μL), and lymphocytes needed to express CD19, CD23, sIg (weak), and CD5 in the absence of pan–T-cell markers. Five patients enrolled on the study were excluded from analysis (diagnosis: large cell lymphoma, marginal zone lymphoma, small lymphocytic lymphoma, Crohn's disease, and CLL with concurrent acute myelogenous leukemia). Three posttreatment patient samples gave insufficient DNA for analysis and thus were excluded from analysis. The study was approved by the University of Michigan Institutional Review Board (IRBMED 2004-0962), and written informed consent was obtained from all patients before enrollment. All analyses were performed on samples obtained during initial enrollment. Follow-up times were calculated from enrollment dates to clinical data analysis date (September 2007). Disease durations at enrollment were calculated from diagnosis dates to enrollment dates.

Cell Isolation

Cell purification. Peripheral blood mononuclear cells from CLL patients were isolated by Ficoll-Paque gradient centrifugation (GE Healthcare), aliquoted into FCS with 10% DMSO, and cryopreserved in liquid nitrogen.

Flow cytometry. Cryopreserved CLL cells were washed and stained with phycoerythrin-conjugated anti-CD19 and FITC-conjugated anti-CD3 antibodies (eBioscience). Propidium iodide was added to a concentration of 1 μg/mL, and viable $CD19^+$ and $CD3^+$ single-positive cells were sorted on a high-speed FACSAria (Becton Dickinson) sorter.

Array Data Analysis

Affymetrix data files were generated from SNP chips posthybridization via scanners at the University of Michigan Microarray Core Facility and imported into the Affymetrix GCOS and GDAS software suites. dChip used native Affymetrix .CEL files and text formatted .CHP files from GDAS to generate copy number heatmap displays (29).

The loss of heterozygosity (LOH) tool was used to display SNPs with LOH between paired tumor samples and buccal DNA (30).

Genomic Southern Blotting

Cryopreserved peripheral blood mononuclear cells derived from CLL patients were washed and then treated with anti-human CD3 (Miltenyi Biotec 130-050-101) and anti-human CD14 microbeads (Miltenyi Biotec 130-050-201) per manufacturer's recommendations. Cell suspensions were run through Miltenyi MACS separation LS columns (130-042-401) to negatively enrich for $CD19^+$ B cells. This resulted in >95% $CD19^+$-positive cells.

Genomic DNA was prepared using digestion of cell pellets with proteinase K at 20 μg/mL in 100 mmol/L Tris, 50 mmol/L EDTA, 50 mmol/L NaCl, and 1% SDS at 56°C. DNA was digested and prepared for Southern analysis using standard protocols.

Probes for genomic Southern analysis were generated using PCR, subcloned into TOPO-TA cloning vectors (Invitrogen) and gel purified. Probes were labeled with α-^{32}P-dCTP using the RadPrime DNA labeling system kit (Invitrogen).

Genomic probes used were composed of ~1.0 to 1.5 kb of DNA corresponding to genomic sequence (green asterisks, probes 1–8; see Fig. 2*C*) including rs9316482 (probe 1), the *miR16/15a* locus (probe 2), rs9316484 (probe 3), *DLEU7-Ex2* (probe 4), *DLEU7-Ex1* (probe 5), physical position 50.382 (probe 6), rs768015 (probe 7), and rs2408291 (probe 8).

Densitometry Analysis for DNA and Protein Quantitation

Film images from Southern or Western blots were obtained using an Alpha Innotech transilluminator and analyzed using the Spot Denso feature of Alpha Ease FC image processing software with background subtraction. Band values were indexed. The reciprocal of all indexed actin band values was computed and then multiplied to the respective analyte band intensity value.

Determination of Immunoglobulin Heavy Chain Variable Gene Mutation Status

Determination of immunoglobulin heavy chain variable gene (IgV_H) mutation status was done as described (31).

Determination of Percentage of ZAP-70–Positive Cells Using Multivariable Fluorescence-Activated Cell Sorting Analysis

Determination of percentage of ZAP-70–positive cells using multivariable fluorescence-activated cell sorting (FACS) analysis was done as described (31).

Fluorescence *In situ* Hybridization

FISH was performed for all patient samples at the Mayo Clinic as a routine clinical test with the following published chromosomal target regions: 6 cen (D6Z1), 6q23.3 (c-myb locus), 11 cen (D11Z1), 11q13 (CCND1-XT), 11q22.3 (ATM), 12 cen (D12Z3), 12q15 (MDM2), 13q14 (D13S319), 13q34 (LAMP1), 14q32 (IGH-XT), 17 cen (D17Z1), 17p13.1 (p53).

Preparation of Sample DNA for Hybridization to Affymetrix 50k-*Xba*I Mapping Arrays and Assay Characteristics

A novel oligonucleotide platform, the 50k SNP chip, was introduced in 2004 by Affymetrix. Selected technical characteristics of the 50k SNP chips are a total combined number of ~58,000 SNPs, a median intermarker distance of ~16 kb, a mean intermarker distance of 47 kb, and average heterozygosity of 0.29.

A 50k SNP chip-based analysis using DNA purified from FACS-sorted $CD19^+$ or $CD3^+$ cells or buccal swabs was done as described (31).

Preparation of CLL-Derived Amplified RNA for Hybridization to Affymetrix Human 133 2.0 Plus Arrays

Twenty $CD19^+$ selected CLL samples were sorted to purity using a high-speed FACSAria (Becton Dickinson) sorter, and RNA was extracted using the Trizol reagent. RNA was further purified using the RNeasy kit (Qiagen). Total RNA (50 ng) was amplified using Ovation RNA Amplification System (NuGen, Inc.), labeled with the FL-Ovation cDNA Biotin module (NuGen, Inc.), and hybridized to the Human 133 2.0 Plus GeneChip (Affymetrix) following the manufacturer's recommended protocols.

Affymetrix GeneChip data were analyzed as follows. Raw probe-level data were converted to expression measures using the Robust Multiarray Average method, which is implemented in the Affymetrix package of BioConductor (32). Briefly, the raw perfect match probes are first quartile normalized to remove any nonbiological variability. The normalized probe data are then converted to an expression measure (log scale) for each gene on each chip using a robust modeling strategy.

For differential expression analysis relating to 13q14 deletion status, we first removed the bottom 25% of probe sets in terms of overall variability. After this filtering step, 41,007 probe sets remained. We then used two-way ANOVA to identify differentially expressed genes, while accounting for the two-batch design of our expression array experiment. The ANOVA model included main effects for both the deletion status and the experimental batch, with the log-scale gene expression measurements as the dependent variable. The deletion effect on gene expression is isolated in the standardized coefficient estimate (the ratio of the deletion effect estimate to its SE). The standardized deletion effect estimates were then analyzed using a false discovery rate at a cutoff of 10% (33).

It was determined that a standardized deletion effect exceeding 3.3 in magnitude corresponded to a 10% or lower false discovery rate. There were 198 probe sets meeting this criterion. These probe sets are listed in Supplementary Table S7 and sorted by the magnitude of their 13q14 deletion coefficient estimate from the ANOVA.

Expression array data were deposited in the GEO repository (34, 35) with the accession number GSE9250 (GSM234840–GSM234859) and can be accessed at the NCBI Web site.[3]

[3] ftp://ftp.ncbi.nih.gov/pub/geo/DATA/supplementary/series/

Measurement of Gene Expression Using Quantitative PCR

RNA was prepared from 2 to 4 × 10^6 FACS-sorted $CD19^+$ cells from 165 CLL cases using the Trizol reagent and resuspended in 100 μL DEPC-treated water. Complementary DNA (20 μL) was made from ~50 ng of RNA using the Superscript III first strand synthesis kit (Invitrogen) and random priming.

Complementary DNA for microRNA reverse transcriptase quantitative PCR (Q-PCR) was made from ~5 ng of RNA using the TaqMan microRNA reverse transcription kit (Applied Biosystems) and RNA-specific primers.

Primers and TaqMan-based probes were purchased from Applied Biosystems (primers-on-demand). Primer/probe mixtures included LATS2 (Hs00324396_m1), PHLPP (Hs01597866_m1), LPIN1 (Hs00299515_m1), DFNA5 (Hs00189346_m1), SERPINE2 (Hs00299953_m1), ARHGAP20 (Hs00826991_m1), cytochrome B5 (Hs00157217_m1), AQP3 (Hs00185020_m1), SLA2 (Hs00260078_m1), GAPD (Hu GAPD), PGK1 (Hu PGK1), miR16 (Tmol/L 391), miR15a (RT 389), RNU43 (TM 1095), and RNU49 (TM 1005).

Duplicate amplification reactions included primers/probes, TaqMan 2× Universal PCR Master Mix, No AmpErase UNG, and 1 μL of cDNA in a 20-μL reaction volume. Reactions were done on an ABI 7900HT machine. Normalization of relative copy number estimates for RNA species of interest was done with the C_t values for GAPD or PGK1 as reference (C_t mean gene of interest − C_t mean GAPD or PGK1). Comparisons between CLL subgroups were performed though subtractions of means of normalized C_t values.

Similar efficacies of amplification of target genes using primers for LATS2, PHLPP, GAPD and PGK1 or miR16, and RNU49 were verified using 2-fold serial dilutions of cDNA made from cell line–derived RNA over a range of 256-fold dilutions. Data were analyzed using least square regression analysis.

Statistical analysis was done using two-sample t statistics. PCR cycle times x were converted to abundance units via the transform $x \rightarrow 1{,}500 \times 2^{-x}$. These values were subsequently transformed to logarithmic abundance units via the transform $x \rightarrow \log(x + 1)/\log(2)$. The resulting values were approximately symmetrically distributed.

Duplicate amplification reactions for microRNAs included primers/probes, TaqMan 2× Universal PCR Master Mix, No AmpErase UNG, and 1.35 μL of cDNA in a 20-μL reaction volume. Normalization of relative copy

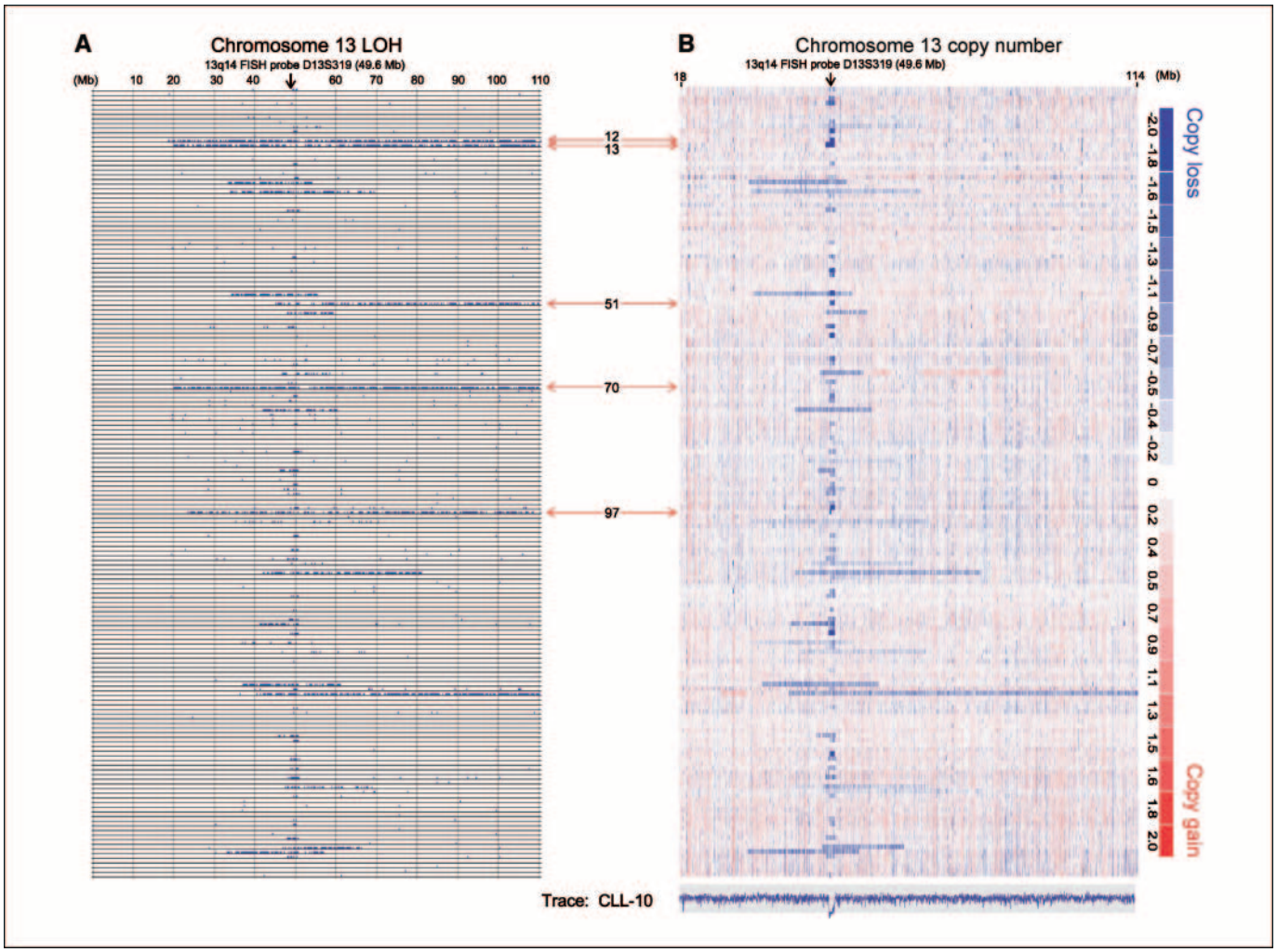

Figure 1. Combined copy number and LOH analysis identifies copy-neutral LOH and significant anatomic variation of del13q14 in CLL. Text files generated through use of the Affymetrix program Copy Number Tool for all patients were imported into the LOH tool, and all individual positions of LOH between buccal DNA and paired tumor DNA were graphed as a blue tick mark across the length of the chromosomes. Copy number estimates for all SNP positions for all patients were generated through dChipSNP as described and displayed across the length of the chromosomes. Copy losses are displayed with blue colors, copy gains with red colors. The physical position of SNPs is not linear along the displayed portions of the chromosome. *A,* LOH display for chromosome 13. Each row represents one patient. *Vertical solid lines,* 10-Mb intervals. The location of the commonly used FISH probe spanning the genomic marker D13S319 at 49.6 Mb physical position is marked with a vertical arrow. *B,* copy number display for chromosome 13. The estimated copy numbers for all SNP positions for CLL 10 are displayed along the entire chromosome below the chromosome 13 display. *Red line,* 2N state; *red double arrows,* CLL patients with copy-neutral LOH (CLLs 12, 13, 51, 70, and 97).

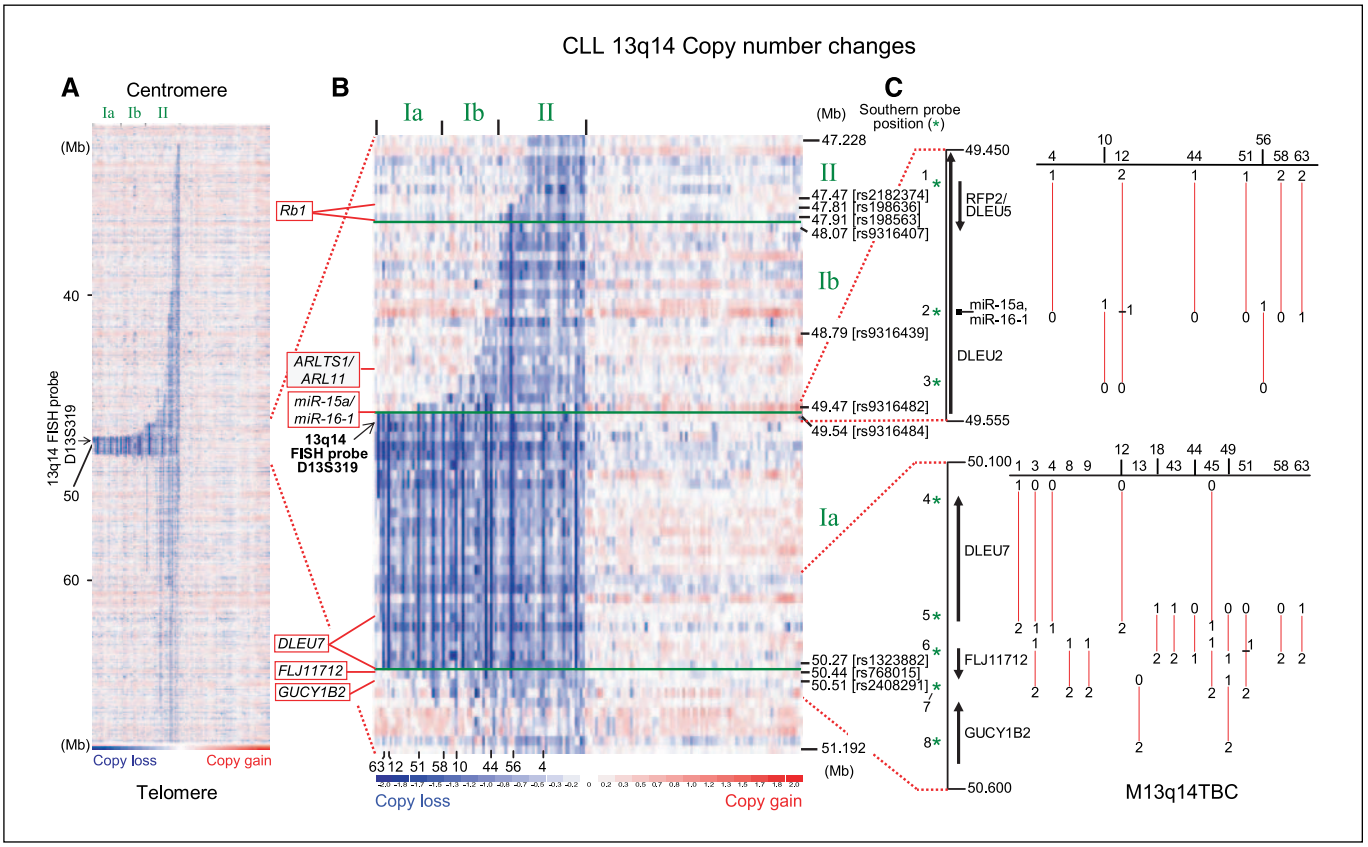

Figure 2. High-resolution analysis of del13q14 identifies subtypes in CLL. Copy number estimates for all SNP positions for all patients for chromosome 13 were generated through dChipSNP as described and displayed across the length of the chromosomes. Copy losses are displayed with blue colors, copy gains with red colors. The physical position of SNPs is not linear along the displayed portions of the chromosome. Each column represents one patient. *A,* clustering of heatmap displays of copy number estimates for all patients for a subregion of chromosome 13 spanning 13q14.3. The location of the commonly used FISH probe spanning the genomic marker D13S319 at 49.6 Mb physical position is marked with an arrow. *B,* clustering of heatmap displays of copy number estimates for all patients for a subregion of chromosome 13 spanning 13q14.3 between physical positions 47.228 and 51.192 Mb. Approximate positions of specific genes are indicated to the left. Proposed subcategories of 13q14.3 deletions are indicated with Roman numerals (types Ia, Ib, and II). *C,* breakpoint mapping for 13q14 type I deletions using genomic Southern blotting. Gene locations and transcriptional orientation are indicated by the vertical black arrows and adjacent gene names. *Green asterisks,* location of probes used for Southern analysis. Individual CLL cases are indicated by black numbers above the black horizontal lines. *Red vertical lines,* region in which a break occurs, with numbers at each end indicating the copy number estimate from quantitative Southern analysis. *Dotted red lines connecting to B,* approximate position of the breaks with regards to the 13q14.3 overview.

number estimates for RNA species of interest was done with the C_t values for the RNU43 or RNU49 as reference (C_t mean gene of interest $-$ C_t mean RNU43 or RNU49). Comparisons between CLL subgroups were performed through subtractions of means of normalized C_t values.

Results

Patient characteristics. Characteristics of the 171 patients analyzed are detailed in Supplementary Tables S1 to S4. Information of familial clustering of the studied cases was not available.

Combined high-resolution LOH and copy number analysis of del13q14 in CLL. 50k SNP array data from 171 patients were analyzed for LOH and subchromosomal copy loss on chromosome 13. Comparative analysis of SNP array–derived detection of del13q14 using copy number analysis compared with clinical FISH results showed strong agreement between both methods: FISH detected 91 of 171 (53%) overall del13q14 incidence and 77 of 171 cases (45%) with >25% of cells involved. SNP arrays detected 82 of 171 del13q14 incidence (48%). SNP arrays detected 74 of 77 (96%) of all CLL cases which were >25% FISH positive and 82 of 91 (90%) of all CLL cases which were FISH positive.

In Fig. 1, we display horizontally LOH data (*A*) for all patients for chromosome 13 together with heatmap displays of paired copy number estimates (*B*). This analysis identified four cases (*red arrows*) with extensive LOH on chromosome 13 but copy loss restricted to a small area at ~D13S319 (~49.6 Mb physical position) and one case without any LOH-associated copy loss (uniparental disomy).

Combined analysis for LOH and copy loss furthermore revealed significant del13q14 lesion length heterogeneity, as well as potential clustering into discrete subtypes, prompting investigation into anatomic and functional differences.

Identification of multiple distinct anatomic subtypes of del13q14 in CLL. Inspection of chromosomal copy number displays for del13q14 at higher resolution led to the characterization of del13q14 subtypes based on anatomic criteria (Fig. 2*A*–*C*). In Fig. 2*A*, we have displayed from left to right all profiled CLL cases according to del13q14 lesion length. In Fig. 2*B*, we display a "zoomed-in" view of the epicenter of these deletions centered on the clinically important genomic FISH probe D13S319. In Fig. 2*C*, we display genomic copy number estimates [red vertical lines flanked by copy number estimates (0, 1, or 2 copies)] based on comparative genomic Southern blotting.

This anatomic clustering allowed us to propose the following schema for del13q14 lesions.

(*a*) Type I lesions (60% of all del13q14 lesions) do not include Rb and almost always terminate in a genomic region at ~50.2 to 50.5 Mb that we, here, term the major 13q14 telomeric breakpoint cluster (*M13q14TBC*; Fig. 2*C*). Within the group of 13q14 type I deletions, one can further identify a majority subset of cases (del13q14 type Ia) with breaks in close proximity to rs9316482 and, therefore, close to the *miR16/15a* locus.

Southern analysis on selected del13q14 type Ia cases (Fig. 2*C*) confirmed that chromosomal breaks occur within a tight genomic region (between 49.45 and 49.55 Mb). Breakpoint analysis further identified cases with bi-allelic loss of the *miR* cluster (physical position at ~49.52 Mb), as well as cases with one retained *miR* cluster copy (Fig. 2*C*). In addition, type Ia lesions were identified in multiple CLL cases coexisting on the second chromosome with larger 13q14 deletions.

(*b*) Type II lesions (40% of all del13q14 lesions) include Rb and, in many cases, extend many Mb past Rb toward the centromere. A subset of type II lesions at the telomeric end terminate in the *M13q14TBC*.

This analysis reliably identified only 2 of 171 CLL cases with deletions shorter than del13q14 type Ia lesions, implying that removal of ~0.8 Mb of chromosomal material from ~49.5 to ~50.5 Mb is required for the biology of del13q14 type Ia lesions (10, 12, 15, 16, 18, 19, 36).

Finally, we note that the clustering of breaks could result in fusion genes in a small subset of CLL cases involving either (*a*) *DLEU2* or either *DLEU7* or *GUCY1B2* or (*b*) *RFP2/DLEU5* and *FLJ11712*.

Clinical characteristics associated with del13q14 subtypes. Of the 171 CLL cases analyzed, 134 were from patients that were untreated at enrollment. Of these 134 patients, 14% had a del13q14 type II, 34% had a del13q14 type I, and 52% lacked a del13q14. The ratio of del13q14 type II to del13q14 type I deletions was 19:46 (0.41). ZAP-70 was positive in 32%, 30%, and 54% of the patients with del13q14 type II, del13q14 type I, or no del13q14, respectively. IgV_H genes were unmutated in 32%, 37%, and 46% of patients with del13q14 type II, del13q14 type I, or no del13q14, respectively (Supplementary Tables S2 and S3A,B; Table 1).

Patients with del13q14 type II showed significantly higher Rai stage at enrollment ($P = 0.02$; linear-by-linear χ^2 test; ref. 37) compared with patients with either del13q14 type I or no del13q14 (mean Rai stage of 1.42, 0.91, and 0.78, respectively). Overall survival data were not mature enough for correlative analysis.

Thirty-seven patients were pretreated at enrollment. Of these 37 patients, 32% had a del13q14 type II, 14% had a del13q14 type I, and 54% lacked a del13q14. The ratio of del13q14 type II to del13q14 type I deletions was 12:5 (2.4; Supplementary Tables S3A,B and S4; Table 1). Interestingly, compared with previously untreated patients, del13q14 type II lesions were significantly enriched and del13q14 type I lesions significantly depleted in the previously treated group of patients ($P = 0.001$).

Finally, of the 46 untreated patients with del13q14 type I, 14 cases displayed copy number estimates of <1 (range, 0.23–0.98; mean, 0.6), whereas 32 cases displayed estimates equal to or >1 (range, 1.0–1.41; mean, 1.17). The Rai stage at enrollment was not significantly different ($P = 0.37$) for these cases (mean Rai stage of 1.1 versus 0.8, respectively).

A subset of CLL cases display very low miR16/miR15a cluster expression. We proceeded to analyze the expression of

Table 1. Summary table of molecular and clinical characteristics of del13q14 subtypes

SNP array–based lesion type	del13q14 type Ia bi-allelic	del13q14 type Ia mono-allelic	del13q14 type Ib	del13q14 type II	Non-del13q14
13q14 Anatomy (Definition)	Centromere break (~rs9316482) Telomere break (~50.2–50.5 Mb) bi-allelic Often includes *miR16/miR15.1* Does not include *Rb* ~13% of all CLL cases	Centromere break (~rs9316482) Telomere break (~50.2–50.5 Mb) mono-allelic Often includes *miR16/miR15.1* Does not include *Rb*	Centromere does not include Rb Telomere variable mono-allelic or bi-allelic Always includes *miR16/miR15.1* Does not include *Rb*	Centromere variable but includes Rb Telomere variable almost always mono-allelic Always includes *miR16/miR15.1* Invariably includes *Rb*	N/A
Lesions incidence (untreated patients)	34% (all type I)	34% (all type I)	34% (all type I)	14%	52%
Lesions incidence (pretreated patients)	14% (all type I)	14% (all type I)	14% (all type I)	32%	54%
Bcl2 expression	High	High	High	High	High
LATS2 expression	Low	Low	Low	Moderate	Moderate
PHLPP expression	Absent in >50% of cases	Absent in >50% of cases	Absent in >50% of cases	Absent in >50% of cases	Variable depending upon type
miR16/miR15.1 expression	Very low	Variable	Variable	Variable	Variable
Associated with prior therapies				Yes, highly enriched ($P = 0.001$)	Variable depending upon type
Mean Rai stage at enrollment	1.1	0.8	0.8	1.42 ($P = 0.02$)	0.78
% ZAP-70 positive cases	30% (all type I)	30% (all type I)	30% (all type I)	32%	54%
% Unmutated IgVH genes cases	37% (all type I)	37% (all type I)	37% (all type I)	32%	46%

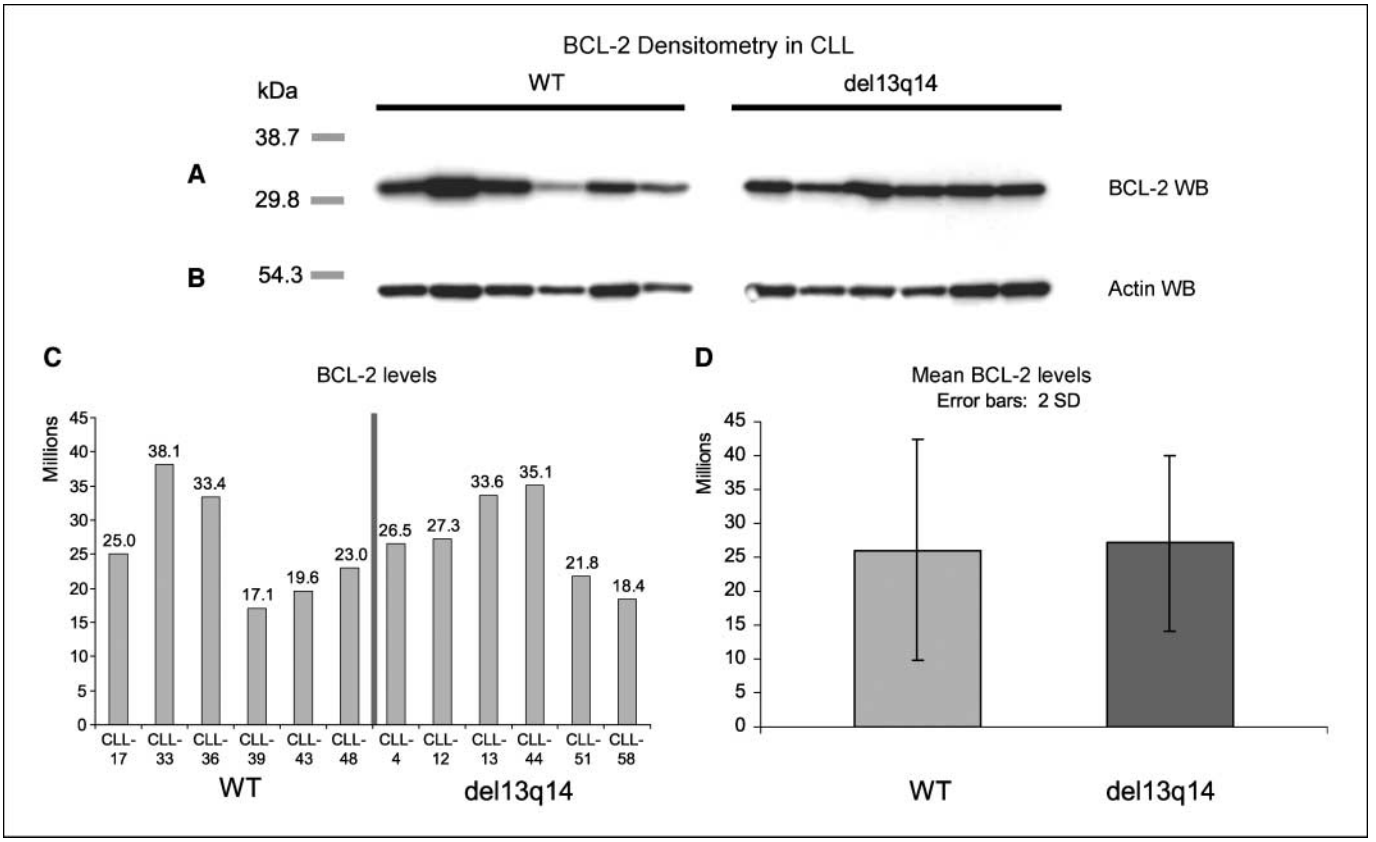

Figure 3. Bcl-2 expression and *miR16/miR15a* levels are not correlated. CD19$^+$ cells from selected CLL cases were sorted to purity using FACS, and cellular lysates were prepared using NP40. Protein was fractionated by SDS-PAGE, transferred to membrane and blotted sequentially with anti–bcl-2 antibodies and anti-actin antibodies. Quantitation was done using imaging software (Materials and Methods). *A,* Bcl-2 immunoblot; *B,* actin immunoblot; *C,* histogram of Bcl-2 levels in genetic subtypes of CLL; *D,* histogram of mean Bcl-2 levels by genetic group.

miR16 and *miR15a* using Q-PCR in ~95% of the 171 CLL cases studied (Supplementary Table S5). Measurements were normalized to expression of two unrelated microRNAs, *RNU43* (on chromosome 22q13.1) and *RNU49* (on chromosome 17p11.2). Expression of *RNU49* and *RNU43* was detected in all CLL cases at relatively uniform levels. The correlation coefficient (with 95% confidence interval) between measurements of RNU49 C_t mean versus RNU43 C_t mean was high at 0.61 (0.51–0.70).

The range of the normalized expression values for both miR16 and miR15a across this large cohort of CLL cases was wide: range ΔC_t miR16-RNU43 of 1.7 to −7.4, 10th percentile to 90th percentile of −0.3 to −5.8 (corresponding to a 45-fold expression difference) and range ΔC_t miR15-RNU43 of 9.4 to −2.2, 10th percentile to 90th percentile of −5.7 to 0.0 (corresponding to a 52-fold expression difference).

We proceeded to compare relative expression levels of *miR16* and *miR15a* in two mutually exclusive CLL subgroups: cases with and without del13q14 by FISH. Mean expression values of both miRs were modestly lower (*miR16* = 1.2-fold/1.7-fold and *miR15a* = 1.4-fold/2-fold for RNU49/RNU43 normalization, respectively) in the del13q14 subgroup as opposed to non-del13q14 CLL cases.

Subsequently, we ranked all CLL cases according to chromosomal copy number estimates for a ~0.4 Mb chromosomal region between rs9316484 (centromeric to the *miR16/15a* locus) and rs3118650 (telomeric to the *miR16/15a* locus). We calculated mean normalized expression values for *miR16* and *miR15a* for the 22 (13%) CLL cases with more extensive chromosomal loss (range, 0.23–0.98; mean, 0.6) and the remaining 141 (87%) CLL cases with less extensive or no loss (range, 1.0–2.32; mean, 1.64).

Mean normalized expression values of both *miR16* and *miR15a* were substantially lower (miR16 = 4.3-fold/3-fold and miR15a = 6.5-fold/4.9-fold for RNU49/RNU43 normalization, respectively) in the subgroup with more extensive del13q14 as opposed to the group with less extensive or no del13q14.

Upon removal of these 22 CLL cases (13%) with extensive del13q14 chromosomal loss from analysis, the relative *miR16/15a* expression levels for the remaining 141 (87%) of cases (with del13q14 or without del13q14) were indistinguishable from all cases without del13q14.

Finally, we ranked all CLL cases by normalized *miR16* or *miR15a* expression and analyzed the 41 (25%) cases with the lowest miR expression levels. This analysis disclosed 8 of 14 (*miR15a/miR16*) cases with no detectable alteration at 13q14 by either FISH or SNP array measurements, but low relative expression of the *miR15a/miR16* genes, comparable in magnitude to CLL cases with extensive del13q14.

This combined data suggests that ~15% of CLL cases indeed have very low miR16/miR15a levels and that the majority of CLL cases (~85%) display a range of expression of these miRs that seems independent of the genetic background.

***MiR16/miR15a* levels do not predict Bcl2 levels in CLL.** Bcl-2 mRNA has been proposed as a physiologic target for miR15a and

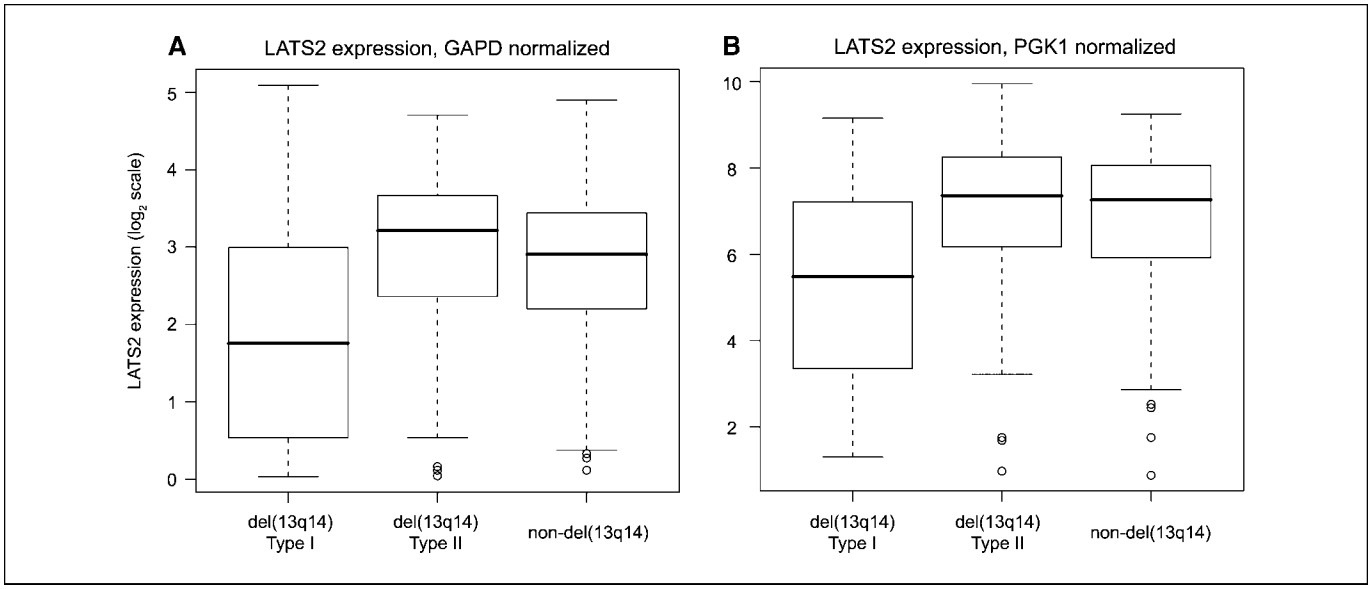

Figure 4. LATS2 expression is lower in CLL 13q14 type I than in other 13q14 subtypes or non-13q14 CLL cases. RNA was prepared from FACS-sorted $CD19^+$ cells from 165 CLL cases. Complementary DNA was made from RNA using the Superscript III first strand synthesis kit (Invitrogen) and random priming. Relative abundance of mRNA for *LATS2* was measured by Q-PCR using the C_t method and normalized to C_t values for GAPD or PGK1. Comparisons between genetic groups were done through comparisons of the normalized C_t means. PCR cycle times x were converted to abundance units via the transform $x \rightarrow 1{,}500 \times 2^{-x}$. These values were subsequently transformed to logarithmic abundance units via the transform $x \rightarrow \log(x + 1)/\log(2)$. The resulting values were approximately symmetrically distributed. Two-sample t tests were used for comparing mean expression between del13q14 type I and type II and non-del13q14 cases. Depicted are box plots for relative expression of *LATS2*. *Horizontal bars,* median. The box comprises the 25th percentile to 75th percentile. Grouping is done according to del13q14 subtype (type I, type II, or non-del13q14). Data based on GAPD and PGK1 normalization.

miR16 in CLL. We therefore measured and compared expression levels of Bcl-2 using immunoblotting in FACS-sorted, highly pure CLL cells derived from CLL cases with or without del13q14 by both FISH and SNP arrays (average copy number estimates of 0.42 versus 2.1) and low versus high relative *miR16/miR15a* expression (ΔC_t *miR16-RNU43* = 0.1 versus −2.5, corresponding to a 6.1-fold expression difference and ΔC_t *miR15-RNU43* = 5.5 versus 2.8, corresponding to a 6.5-fold expression difference).

As can be seen in Fig. 3*A-C*, Bcl-2 levels, once normalized to Actin levels, were similar in both groups of CLL cases, prompting our interest in other genes deregulated as a consequence of del13q14.

Identification of deregulated genes in CLL cases with del13q14 type I. To identify genes deregulated in CLL cases with del13q14 type Ia, we selected 10 CLL cases each with and without this lesion type and sorted $CD19^+$ cells to purity using FACS sorting. Characteristics of the CLL cases profiled are summarized in Supplementary Table S6. We subsequently measured expression levels of preamplified RNA species using the Affymetrix Human 133 2.0 Plus arrays. Data were analyzed as described in Materials and Methods. All 198 genes, ranked in Supplementary Table S7 by the magnitude of the expression difference, displayed a false-discovery rate of <0.1.

In this group of 198 genes, we identified reduced expression of *FLJ11712, KCNRG, RFP2, RFP2OS*, and *DLEU1*, providing confidence that genes deleted through del13q14 type I displayed reduced relative expression under our assay conditions.

Multiple other genes emerged as candidate differentially expressed genes from this analysis. Measurements of expression of *LATS2, DFNA5, PHLPP, LPIN1, SERPINE2, ARHGAP20, CYTB5, SLA2,* and *AQP3* by Q-PCR in cDNA derived from the 20 CLL samples used for array analysis confirmed differential expression of these genes (see Supplementary Table S8).

LATS2 showed substantial and significant underexpression in del13q14 cases as opposed to reference cases as detected by two probes and was one of the genes selected for further study (Supplementary Fig. S1).

Finally, PHLPP, a recently discovered phosphatase that dephosphorylates Ser^{473} in AKT was selected for study as differential AKT activity and/or expression in CLL has been described (3, 38).

***LATS2* expression levels are lower in CLL with del13q14 type I as opposed to all other CLL types.** *LATS2* expression levels were measured in 165 CLL cases using Q-PCR, and data were normalized using either *GAPD* or *PGK1* expression levels (Supplementary Table S9). Expression of *GAPD* and *PGK1* was detected in all CLL cases at relatively uniform levels. The correlation coefficient (with 95% confidence interval) between measurements of GAPD C_t mean versus PGK1 C_t mean was high at 0.78 (0.72–0.84).

Analysis of LATS2 levels by subgroups showed 1.6-fold/1.7-fold (GAPD/PGK1 normalization) lower expression levels in CLL cases with del13q14 than in all cases without del13q14. Given that we had initially observed the differential expression of *LATS2* in del13q14 type Ia lesions as opposed to non-del13q14 cases, we proceeded to analyze *LATS2* expression in three distinct CLL groups: (*a*) CLL with del13q14 type I, (*b*) CLL with del13q14 type II, and (*c*) all other CLL cases.

Interestingly, this analysis uncovered that CLL cases with del13q14 type I showed reduced *LATS2* expression relative to CLL cases with del13q14 type II (~2.6-fold/~2.8-fold of GAPD/PGK1 normalization, respectively) or no del13q14 (~2.6-fold/~2.6-fold of GAPD/PGK1 normalization, respectively; ΔC_t mean LATS2-GAPD of 9.8/8.4/8.4, respectively, and ΔC_t mean LATS2-PGK1 of 5.4/3.9/3.8, respectively; Fig. 4*A* and *B*).

These differences were highly statistically significant [P values of 0.003 (GAPD) and 0.011 (PGK1) for comparison of type I and type II

del13q14 lesions and 0.001 (GAPD) and 0.0003 (PGK1) for comparison of type I and non-del13q14 cases using two sample *t* testing].

***PHLPP* expression is low or undetectable in ~50% of CLL cases with del13q14.** Q-PCR–based measurements of *PHLPP* expression in the 20 CLL cases profiled using the expression arrays detected low/absent expression in 8 of 10 of the del13q14 cases versus 3 of 10 of the reference cases (Supplementary Table S8).

Subsequently, *PHLPP* expression levels were measured in 164 CLL cases using Q-PCR, and data were normalized using *PGK1* expression levels. CLL cases with a ΔC_t (C_t mean PHLPP $-$ C_t mean PGK1) of >9 (indicating very low relative levels) or cases with undetectable levels were grouped as low/absent *PHLPP* expression (Supplementary Table S10).

Correlative analysis of *PHLPP* expression by FISH categories discovered that ~50% of CLL cases with del13q14 did not express *PHLPP* (Fig. 5). The percentage of CLL cases that did not express *PHLPP* was 51% (isolated del13q14), 40% (normal FISH), 28% (complex FISH), 22% (isolated del11q or del17p), and 14% (isolated trisomy 12), respectively. Using a standard test of proportions, the difference between del13q14 and trisomy 12 cases for *PHLPP* expression was highly significant at P of 0.01, whereas a trend was observed for the comparison of del13q14 and complex FISH findings ($P = 0.14$).

Deletion 13q14 in CLL comprises multiple subtypes. A summary of the distinct molecular and clinical characteristics of the newly identified del13q14 subtypes in CLL has been tabulated in Table 1.

Discussion

In this study, we describe the results of a high-resolution analysis of del13q14 in a large cohort of CLL patients using high-density SNP oligonucleotide arrays. SNP arrays offer an unbiased approach to the evaluation of entire cancer genomes through the assessment of allelic losses/gains and LOH (39–41).

A significant strength of this study is the use of sorted $CD19^+$ cells as substrates for all analyses, effectively eliminating confounding variables introduced by non–B cells.

SNP array analysis proved to be a highly sensitive and specific method for determining copy number losses at 13q14 in CLL based on comparison with FISH. Both methods, with few exceptions, detected the same cases.

Detailed anatomic analysis of del13q14 suggested to us the existence of distinct subtypes. Our initial suggestion for categorization classifies del13q14 lesions with Rb loss as type II (40% of del13q14 cases) and without such loss as type I (60% of del13q14 cases). Rb is a critical regulator of cell cycle progression and genomic stability, and loss of one or two alleles could differentially affect the biology of affected CLL cases (42, 43); further support for clustering del13q14 type I lesions as a separate group comes from expression analysis of *LATS2*, which we performed across this large CLL cohort.

LATS2 RNA levels were found to be low in CLL cases with del13q14 type I as opposed to type II cases or all other CLL cases without del13q14. Given that LATS2 has been implicated in cell cycle progression control, we surmise that Rb, LATS2, and possibly additional, unidentified regulators (in non-del13q14 cases) are regulating this process in different subsets of CLL (44, 45).

The mechanism of low *LATS2* expression in CLL subtypes is not known; *LATS2* lies outside of all 13q14 deletions. Possibilities include *LATS2* promoter methylation, as described for other cancers, or an effect in *trans* of 13q14 resident genes on *LATS2* expression (46, 47).

The discovery of differing LATS2 levels in CLL subtypes may also be of interest in the context of response to therapy or disease progression, as LATS2 has been shown to intersect with the Mdm2-p53 axis (48). This topic needs prospective analysis in well-defined CLL cohorts.

Further subdivision of del13q14 type I cases into type Ia and type Ib is suggested by the occurrence of deletions that appear of relatively uniform length (del13q14 type Ia) and that display centromeric breaks within the vicinity of the *miR15a/miR16* cluster and telomeric breaks within a newly identified break cluster that we here term the major telomeric del13q14 breakpoint cluster. Bi-allelic del13q14 type Ia lesions were associated with marked reductions in *miR15a/miR16* expression levels and

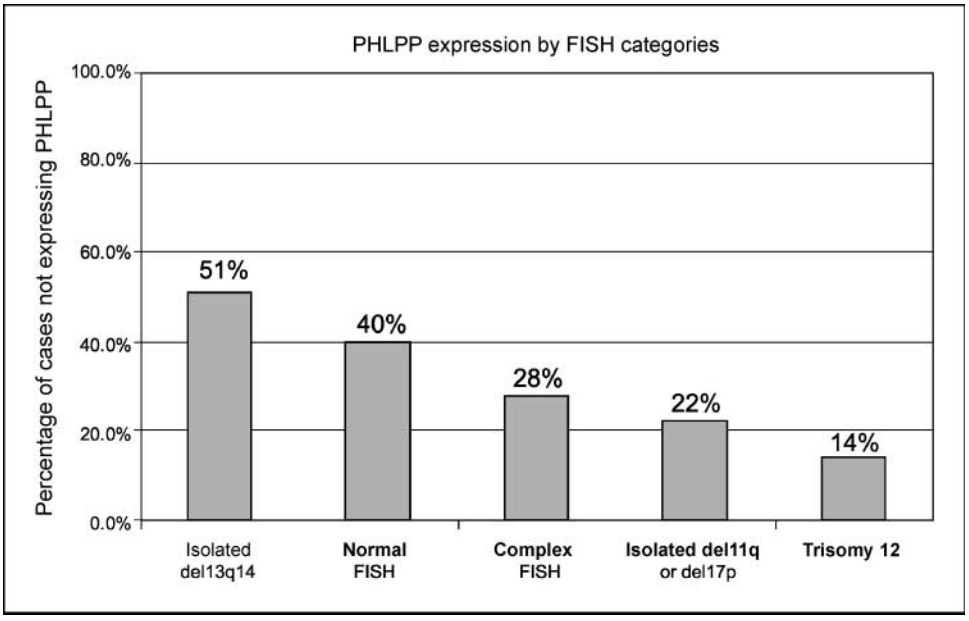

Figure 5. *PHLPP* is not expressed in ~50% of CLL cases with del13q14. RNA was prepared from FACS-sorted $CD19^+$ cells from 164 CLL cases. Complementary DNA was made from RNA using the Superscript III first strand synthesis kit (Invitrogen) and random priming. Relative abundance of mRNA for *PHLPP* was measured by Q-PCR using the C_t method and normalized to C_t values for PGK1. Depicted is the percentage of CLL cases in the indicated FISH-based genetic categories [isolated del13q14, normal FISH, complex FISH (more than one FISH abnormality), isolated del11q or del17p, and trisomy 12] that had very low or absent PHLPP expression.

may exert effects on affected CLL cases through yet-to-be identified *miR15a/miR16* targets. In this context, it seems relevant that Bcl-2 levels were not correlated with *miR15a/miR16* levels, providing a renewed impetus for searches for critical miR15a/miR16 targets (26).

Correlative analysis of surrogate clinical end points/variables by del13q14 subtype disclosed a higher Rai stage at study enrollment for del13q14 type II lesions, as opposed to del13q14 type I lesions. Furthermore, we detected a highly significant enrichment for del13q14 type II cases in previously treated as opposed to untreated CLL specimens. Whereas these data may portend that del13q14 type II is a marker for more aggressive CLL, only prospectively collected clinical data will allow for firm conclusions to be drawn regarding possible detrimental effects of del13q14 type II lesions on CLL outcome.

The novel discovery that ~50% of all CLL cases with del13q14 do not express *PHLPP* is of interest. PHLPP dephosphorylates activated AKT and low or absent *PHLPP* expression may allow for sustained AKT signaling after proper cell surface stimuli (49).

In summary, anatomic and functional data suggest that multiple genes are deregulated as part of various deletions on chromosome 13, including genes with properties that warrant reduction in actively dividing cancer cells (*Rb, LATS2*) and genes with the potential for more specialized functions (*miR15a/miR16, RFP2, PHLPP* and others; ref. 50).

Acknowledgments

Received 8/13/2007; revised 11/19/2007; accepted 12/6/2007.

Grant support: Leukemia and Lymphoma Society of America Special Fellow Award (S. Malek), Leukemia Research Foundation New Investigator Award (S. Malek), NIH grant 1R21 CA124420-01A1 (S. Malek), and NIH through University of Michigan's Cancer Center support grant 5 P30 CA46592.

The costs of publication of this article were defrayed in part by the payment of page charges. This article must therefore be hereby marked *advertisement* in accordance with 18 U.S.C. Section 1734 solely to indicate this fact.

References

1. Chiorazzi N, Rai KR, Ferrarini M. Chronic lymphocytic leukemia. N Engl J Med 2005;352:804–15.
2. Grever MR, Lucas DM, Dewald GW, et al. Comprehensive assessment of genetic and molecular features predicting outcome in patients with chronic lymphocytic leukemia: results from the US Intergroup Phase III Trial E2997. J Clin Oncol 2007;25:799–804.
3. Kienle DL, Korz C, Hosch B, et al. Evidence for distinct pathomechanisms in genetic subgroups of chronic lymphocytic leukemia revealed by quantitative expression analysis of cell cycle, activation, and apoptosis-associated genes. J Clin Oncol 2005;23:3780–92.
4. Mayr C, Speicher MR, Kofler DM, et al. Chromosomal translocations are associated with poor prognosis in chronic lymphocytic leukemia. Blood 2006;107:742–51.
5. Juliusson G, Oscier DG, Fitchett M, et al. Prognostic subgroups in B-cell chronic lymphocytic leukemia defined by specific chromosomal abnormalities. N Engl J Med 1990;323:720–4.
6. Dohner H, Stilgenbauer S, Benner A, et al. Genomic aberrations and survival in chronic lymphocytic leukemia. N Engl J Med 2000;343:1910–6.
7. Chen C, Frierson HF, Jr., Haggerty PF, Theodorescu D, Gregory CW, Dong JT. An 800-kb region of deletion at 13q14 in human prostate and other carcinomas. Genomics 2001;77:135–44.
8. Liu Y, Hermanson M, Grander D, et al. 13q deletions in lymphoid malignancies. Blood 1995;86:1911–5.
9. Rowntree C, Duke V, Panayiotidis P, et al. Deletion analysis of chromosome 13q14.3 and characterisation of an alternative splice form of LEU1 in B cell chronic lymphocytic leukemia. Leukemia 2002;16:1267–75.
10. Wolf S, Mertens D, Schaffner C, et al. B-cell neoplasia associated gene with multiple splicing (BCMS): the candidate B-CLL gene on 13q14 comprises more than 560 kb covering all critical regions. Hum Mol Genet 2001;10:1275–85.
11. Rondeau G, Moreau I, Bezieau S, et al. Comprehensive analysis of a large genomic sequence at the putative B-cell chronic lymphocytic leukaemia (B-CLL) tumour suppresser gene locus. Mutat Res 2001;458:55–70.
12. Migliazza A, Bosch F, Komatsu H, et al. Nucleotide sequence, transcription map, and mutation analysis of the 13q14 chromosomal region deleted in B-cell chronic lymphocytic leukemia. Blood 2001;97:2098–104.
13. Mabuchi H, Fujii H, Calin G, et al. Cloning and characterization of CLLD6, CLLD7, and CLLD8, novel candidate genes for leukemogenesis at chromosome 13q14, a region commonly deleted in B-cell chronic lymphocytic leukemia. Cancer Res 2001;61:2870–7.
14. Bullrich F, Fujii H, Calin G, et al. Characterization of the 13q14 tumor suppressor locus in CLL: identification of ALT1, an alternative splice variant of the LEU2 gene. Cancer Res 2001;61:6640–8.
15. Kitamura E, Su G, Sossey-Alaoui K, et al. A transcription map of the minimally deleted region from 13q14 in B-cell chronic lymphocytic leukemia as defined by large scale sequencing of the 650 kb critical region. Oncogene 2000;19:5772–80.
16. Kapanadze B, Makeeva N, Corcoran M, et al. Comparative sequence analysis of a region on human chromosome 13q14, frequently deleted in B-cell chronic lymphocytic leukemia, and its homologous region on mouse chromosome 14. Genomics 2000;70:327–34.
17. Liu Y, Corcoran M, Rasool O, et al. Cloning of two candidate tumor suppressor genes within a 10 kb region on chromosome 13q14, frequently deleted in chronic lymphocytic leukemia. Oncogene 1997;15:2463–73.
18. Kalachikov S, Migliazza A, Cayanis E, et al. Cloning and gene mapping of the chromosome 13q14 region deleted in chronic lymphocytic leukemia. Genomics 1997;42:369–77.
19. Bouyge-Moreau I, Rondeau G, Avet-Loiseau H, et al. Construction of a 780-kb PAC, BAC, and cosmid contig encompassing the minimal critical deletion involved in B cell chronic lymphocytic leukemia at 13q14.3. Genomics 1997;46:183–90.
20. Corcoran MM, Hammarsund M, Zhu C, et al. DLEU2 encodes an antisense RNA for the putative bicistronic RFP2/LEU5 gene in humans and mouse. Genes Chromosomes Cancer 2004;40:285–97.
21. Mertens D, Wolf S, Schroeter P, et al. Down-regulation of candidate tumor suppressor genes within chromosome band 13q14.3 is independent of the DNA methylation pattern in B-cell chronic lymphocytic leukemia. Blood 2002;99:4116–21.
22. Calin GA, Dumitru CD, Shimizu M, et al. Frequent deletions and down-regulation of micro-RNA genes miR15 and miR16 at 13q14 in chronic lymphocytic leukemia. Proc Natl Acad Sci U S A 2002;99:15524–9.
23. Cimmino A, Calin GA, Fabbri M, et al. miR-15 and miR-16 induce apoptosis by targeting BCL2. Proc Natl Acad Sci U S A 2005;102:13944–9.
24. Nuckel H, Frey UH, Bau M, et al. Association of a novel regulatory polymorphism (-938C>A) in the BCL2 gene promoter with disease progression and survival in chronic lymphocytic leukemia. Blood 2007;109:290–7.
25. Matsuzaki H, Dong S, Loi H, et al. Genotyping over 100,000 SNPs on a pair of oligonucleotide arrays. Nat Methods 2004;1:109–11.
26. Fulci V, Chiaretti S, Goldoni M, et al. Quantitative technologies establish a novel microRNA profile of chronic lymphocytic leukemia. Blood 2007;109:4944–51.
27. Gao T, Furnari F, Newton AC. PHLPP: a phosphatase that directly dephosphorylates Akt, promotes apoptosis, and suppresses tumor growth. Mol Cell 2005;18:13–24.
28. Cheson BD, Bennett JM, Grever M, et al. National Cancer Institute-sponsored Working Group guidelines for chronic lymphocytic leukemia: revised guidelines for diagnosis and treatment. Blood 1996;87:4990–7.
29. Lin M, Wei LJ, Sellers WR, Lieberfarb M, Wong WH, Li C. dChipSNP: significance curve and clustering of SNP-array-based loss-of-heterozygosity data. Bioinformatics 2004;20:1233–40.
30. Ross CW, Ouillette PD, Saddler CM, Shedden KA, Malek SN. Comprehensive analysis of copy number and allele status identifies multiple chromosome defects underlying follicular lymphoma pathogenesis. Clin Cancer Res 2007;13:4777–85.
31. Saddler C, Ouillette P, Kujawski L, et al. Comprehensive biomarker and genomic analysis identifies P53 status as the major determinant of response to MDM2 inhibitors in chronic lymphcytic leukemia. Blood. In press 2008.
32. Irizarry RA, Bolstad BM, Collin F, Cope LM, Hobbs B, Speed TP. Summaries of Affymetrix GeneChip probe level data. Nucleic Acids Res 2003;31:e15.
33. Storey JD. A direct approach to false discovery rates. J R Stat Soc Ser B Meth 2002;64:479–98.
34. Barrett T, Troup DB, Wilhite SE, et al. NCBI GEO: mining tens of millions of expression profiles-database and tools update. Nucleic Acids Res 2007;35:D760–5.
35. Edgar R, Domrachev M, Lash AE. Gene Expression Omnibus: NCBI gene expression and hybridization array data repository. Nucleic Acids Res 2002;30:207–10.
36. Hammarsund M, Corcoran MM, Wilson W, et al. Characterization of a novel B-CLL candidate gene-DLEU7-located in the 13q14 tumor suppressor locus. FEBS Lett 2004;556:75–80.
37. Agresti A. A survey of models for repeated ordered categorical response data. Stat Med 1989;8:1209–24.
38. Petlickovski A, Laurenti L, Li X, et al. Sustained signaling through the B-cell receptor induces Mcl-1 and promotes survival of chronic lymphocytic leukemia B cells. Blood 2005;105:4820–7.
39. Pfeifer D, Pantic M, Skatulla I, et al. Genome-wide analysis of DNA copy number changes and LOH in CLL using high-density SNP arrays. Blood 2007;109:1202–10.
40. Raghavan M, Lillington DM, Skoulakis S, et al. Genome-wide single nucleotide polymorphism analysis

reveals frequent partial uniparental disomy due to somatic recombination in acute myeloid leukemias. Cancer Res 2005;65:375–8.
41. Zhao X, Li C, Paez JG, et al. An integrated view of copy number and allelic alterations in the cancer genome using single nucleotide polymorphism arrays. Cancer Res 2004;64:3060–71.
42. Pickering MT, Kowalik TF. Rb inactivation leads to E2F1-mediated DNA double-strand break accumulation. Oncogene 2006;25:746–55.
43. Hernando E, Nahle Z, Juan G, et al. Rb inactivation promotes genomic instability by uncoupling cell cycle progression from mitotic control. Nature 2004;430:797–802.
44. Yabuta N, Okada N, Ito A, et al. Lats2 is an essential mitotic regulator required for the coordination of cell division. J Biol Chem 2007;282:19259–71.
45. Chan EH, Nousiainen M, Chalamalasetty RB, Schafer A, Nigg EA, Sillje HH. The Ste20-like kinase Mst2 activates the human large tumor suppressor kinase Lats1. Oncogene 2005;24:2076–86.
46. Jiang Z, Li X, Hu J, et al. Promoter hypermethylation-mediated down-regulation of LATS1 and LATS2 in human astrocytoma. Neurosci Res 2006;56:450–8.
47. Takahashi Y, Miyoshi Y, Takahata C, et al. Down-regulation of LATS1 and LATS2 mRNA expression by promoter hypermethylation and its association with biologically aggressive phenotype in human breast cancers. Clin Cancer Res 2005;11:1380–5.
48. Aylon Y, Michael D, Shmueli A, Yabuta N, Nojima H, Oren M. A positive feedback loop between the p53 and Lats2 tumor suppressors prevents tetraploidization. Genes Dev 2006;20:2687–700.
49. Ticchioni M, Essafi M, Jeandel PY, et al. Homeostatic chemokines increase survival of B-chronic lymphocytic leukemia cells through inactivation of transcription factor FOXO3a. Oncogene 2007;26:7081–91.
50. Messmer BT, Messmer D, Allen SL, et al. *In vivo* measurements document the dynamic cellular kinetics of chronic lymphocytic leukemia B cells. J Clin Invest 2005;115:755–64.

Integrated Genomic Profiling of Chronic Lymphocytic Leukemia Identifies Subtypes of Deletion 13q14

Peter Ouillette, Harry Erba, Lisa Kujawski, et al.

Cancer Res 2008;68:1012-1021.